

# Atlantis — 20 years of seismic innovation finally removes the shroud of mystery



Sam Buist<sup>1</sup>, Li Jiang<sup>1</sup>, Obi Egbue<sup>1</sup>, Daniel Tebo<sup>1</sup>, Luis Lopez<sup>1</sup>, Zhiyuan Wei<sup>2</sup>, Alex Hao<sup>2</sup>, and Chi Chen<sup>2</sup>

<https://doi.org/10.1190/tle42060406.1>

## Abstract

The Atlantis Field has gone through more than two decades of continuous seismic imaging efforts, during which time many innovative technologies were incubated, the most recent one being the successful application of full-waveform inversion (FWI) in salt environments. This technique led to a significant improvement in the subsalt image. However, imaging challenges remain for the Atlantis reservoirs, primarily due to the complex overburden salt geometries and the highly compartmentalized reservoir. Even with an improved velocity model from FWI, the conventional reverse time migration (RTM) images still suffer from illumination issues and contain strong migration swings that hinder the subsalt imaging and subsequent interpretations. Furthermore, early versions of FWI employed an acoustic assumption, leading to visible salt halos at the salt boundaries in the velocity model, which adversely impacted the reservoir imaging. In the last 12 months, elastic time-lag FWI (TLFWI) and FWI-derived reflectivity (FDR) imaging using long-offset ocean-bottom node data have minimized these imaging issues at Atlantis, providing another step change in subsalt understanding. Although the 3D RTM images using the elastic FWI velocity model are similar overall to their acoustic counterparts, the 4D time-lapse RTM images at Atlantis show noticeable improvements. Furthermore, FDR images derived from elastic FWI velocities show obvious benefits over the acoustic ones. With a more accurate modeling engine that allows for better match between synthetic and real data, FDR imaging shows improved illumination, higher signal-to-noise ratio, and better reservoir details over acoustic FDR imaging. This recent advancement in using elastic TLFWI has had immediate positive effects in facilitating the Atlantis Field's current and future development.

## Introduction

The Atlantis Field, one of BP's major developments in the Gulf of Mexico, is located 150 miles south of New Orleans in the southeast Green Canyon area (Figure 1). The footprint of the field straddles the Sigsbee Escarpment, with water depth ranging from 1300 to 2100 m. It was first discovered in 1998, sanctioned in 2002, and put into production in 2007. The field consists of multiple stacked producing reservoirs within a highly

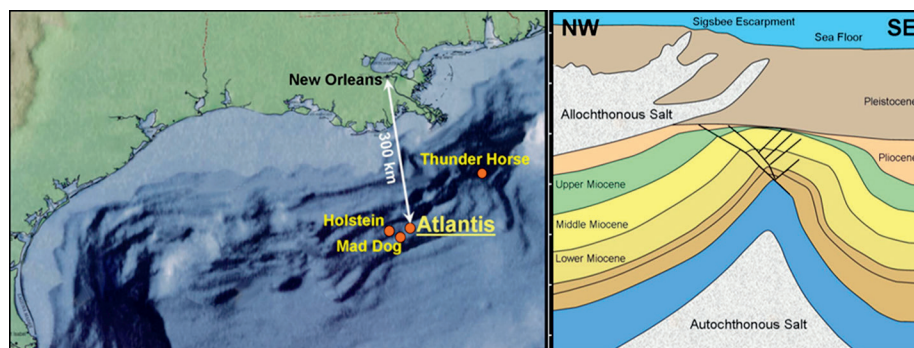


**Figure 1.** (a) Atlantis Field is located in the Green Canyon area of the Gulf of Mexico, 150 miles south of New Orleans. (b) Multiple stacked Miocene reservoirs lie below complex salt bodies.

faulted, four-way, salt-cored anticline. A large portion of the reservoirs (60%) sits underneath the salt canopy, which has evolved into a series of complex allochthonous salt geometries such as tubular thin salt bodies (salt fingers), sediment inclusions, and sutures, all of which pose tremendous challenges to velocity model building and reservoir imaging. On the north side, despite the simpler salt geometry, the steeply dipping salt flanks lead to poor illumination at the reservoir level. Additionally, the highly faulted reservoir structure adds more complexity and difficulties to the imaging.

To improve reservoir imaging and reduce risk in Atlantis Field development, BP has made numerous pioneering technology developments in data acquisition, including the first deepwater full-azimuth ocean-bottom node (OBN) survey in 2005 (Beaudoin and Ross, 2007), followed by four 4D monitor OBN surveys acquired in 2009, 2015, 2019, and 2022. Besides serving 4D monitor purposes, each additional OBN survey was upgraded further by the inclusion of novel technologies to improve the velocity model and image quality. Starting in 2015, the OBN node patch was extended to the north (subsalt) to obtain longer offsets up to 35 km, making it an appropriate data set to update the velocity model with full-waveform inversion (FWI), improving the subsalt illumination (Lewis et al., 2016). In the 2019 and 2022 OBN surveys, the nodes were reduced in the north whereas the receiver density over the core of the field was increased to 200 × 400 m and 200 × 200 m, respectively, aiming to further improve the signal-to-noise ratio (S/N) of the subsalt image by using the increased data density to reduce subsalt noise (van Gestel et al., 2021). Additionally, a low-frequency source called Wolfspar was used in the 2019 OBN acquisition (Dellinger et al., 2016; Brenders et al., 2022) to evaluate the impact of very low frequency data to FWI results.

<sup>1</sup>BP, Houston, Texas, USA. E-mail: sam.buist@bp.com; li.jiang@bp.com; obi.egbue@bp.com; daniel.tebo@bp.com; luis.lopez1@bp.com.

<sup>2</sup>CGG, Houston, Texas, USA. E-mail: zhiyuan.wei@cgg.com; alex.hao@cgg.com; chi.chen@cgg.com.

## Correcting salt velocity errors by acoustic FWI

Each aforementioned data set went through a thorough processing flow using the latest processing technology available at the time. However, the improvements in the Atlantis subsalt areas were only incremental until 2016 when BP had its first breakthrough success using FWI for salt velocity model updating using the long-offset 2015 OBN data. BP's FWI revolutionized the Atlantis salt velocity model building flow and made it less human intensive (Michell et al., 2017; Shen et al., 2017). Prior to this stable FWI workflow for salt, the industry-standard methodology was a top-down approach, based on reflection tomography to update the sediment velocity, followed by sediment and salt floods interleaved with migration and manual picking of top and base of salt. Labor-intensive salt scenario tests were then performed to correct the salt velocity errors. In Atlantis, extensive manual interpretation efforts with hundreds of salt scenarios have been tried over the years. However, it was difficult to resolve the complex salt structure and corresponding velocity perfectly, so the additional man hours returned minimal improvement. With the data-driven FWI workflow, the resulting reverse time migration (RTM) images showed great improvement over legacy images, especially subsalt, once the overburden salt model errors were resolved.

Zhang et al. (2018) built on the progress in FWI shown by Michell et al. (2017) and Shen et al. (2017). Zhang et al. (2018) developed time-lag FWI (TLFWI), which further improves the inversion for the velocity model in complex salt environments. TLFWI uses a time-lag cost function to reduce the

influence of modeled amplitude errors. Furthermore, it uses frequency-dependent time windows for time-lag measurements and the cross-correlation coefficient between recorded data and synthetic data to promote more accurate traveltimes (Zhang et al., 2018; Wang et al., 2019). TLFWI normally can start from a lower frequency than conventional FWI can. This can resolve larger velocity errors and is also essential to mitigate cycle-skipping issues. As shown in Figures 2a and 2b, the 11 Hz acoustic TLFWI corrected large salt model misinterpretations in the legacy model that were built by the conventional top-down velocity model workflows. For example, the complex salt fingers and salt inclusions that are very difficult for manual picking to fully resolve are captured automatically by acoustic TLFWI. As a result, the improved velocity model brings significant improvements to the corresponding RTM image with reduced migration swings and more coherent subsalt reflectors (Figures 2c and 2d).

Despite the improved kinematics from the acoustic TLFWI velocity model where only the  $V_p$  model is updated ( $V_s$  follows an empirical relationship with  $V_p$ , and density is constant throughout), the RTM image still contains swing noise in the subsalt portions of the image due to illumination issues caused by the steeply dipping salt flank to the north, which distorts the wavefronts and impacts the ability to image the underlying reservoir interval with any confidence. These images have a corresponding degraded S/N in these low-illumination zones. FWI-derived reflectivity (FDR) imaging, which employs least-squares fitting of the full wavefield data, is deemed to be a powerful tool to compensate for the illumination issue and improve the subsalt S/N (Zhang et al., 2020; Huang et al., 2021; Wei et al., 2023).

With the kinematic errors better resolved by TLFWI, higher-frequency FDR imaging has delivered its promise in improving the subsalt images in Atlantis. The 18 Hz acoustic FDR image derived from the same 18 Hz acoustic TLFWI velocity model gives the much-improved S/N and event continuity in the same subsalt low-illumination area where the RTM image is suboptimal (Figures 3b and 3c). In the sediment area outboard of salt where the overburden is relatively simple, the dipping reservoir reflectors down the forelimb show a "washed-out" zone (red arrow in Figure 3b). This is due to the limited node coverage and insufficient aperture of the input OBN data. Coupling the full wavefield data (diving wave and surface-related multiple energy) along with the iterative least-squares fitting process, FDR imaging nicely resolves those dipping events with a level of clarity not seen before (green arrow in Figure 3c).

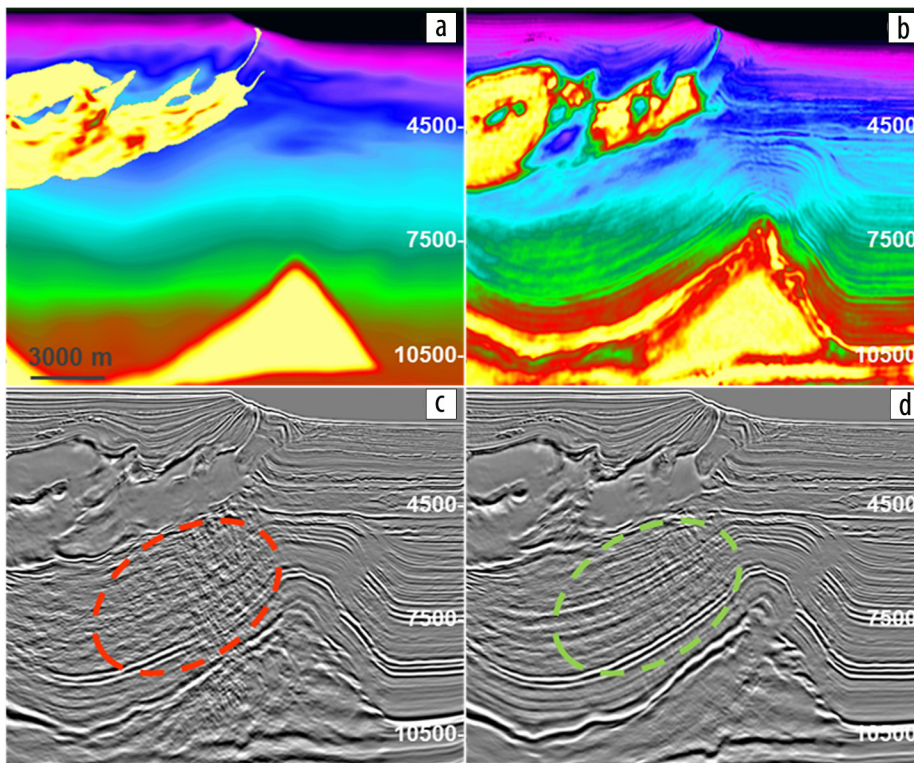


**Figure 2.** Section view of (a) velocity model built from conventional top-down velocity model building flow, (b) 11 Hz acoustic TLFWI velocity model, (c) 20 Hz RTM image migrated with velocity model in (a), and (d) 20 Hz RTM image migrated with acoustic TLFWI.

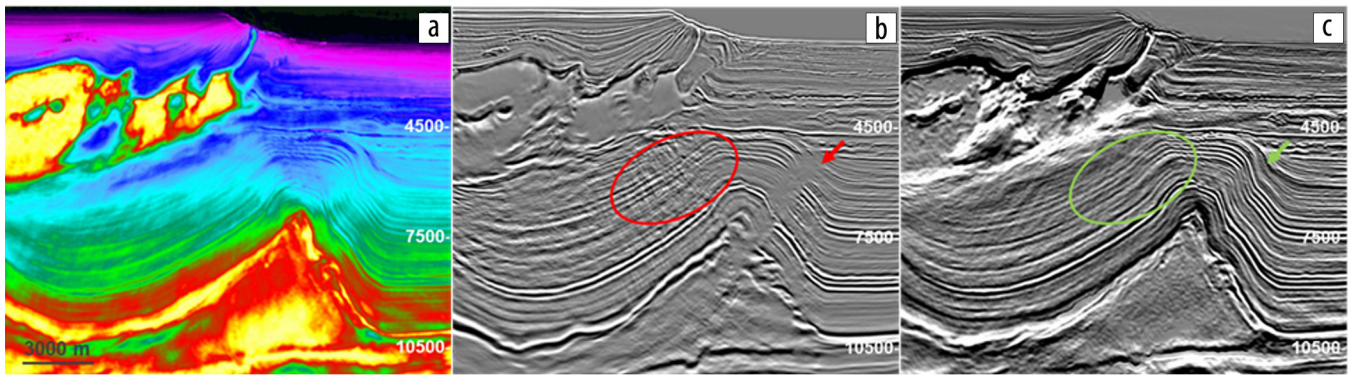


**Figure 3.** Section view of Atlantis acoustic model and images: (a) 18 Hz acoustic TLFWI velocity model, (b) 20 Hz RTM image migrated with 18 Hz acoustic TLFWI velocity model, and (c) 18 Hz acoustic FDR image derived from 18 Hz acoustic TLFWI model in (b).

### Improving Atlantis images by elastic FWI

Although acoustic TLFWI greatly improved the kinematics of the velocity model in Atlantis, the salt halo of the 11 Hz acoustic TLFWI velocity model (Figure 4a) is partially due to the fact that the acoustic approximation cannot produce a modeled wavefield with correct amplitude and phase in a high-contrast solid medium (Elebiju et al., 2022; Wu et al., 2022; Zhang et al., 2023). When the elastic TLFWI workflow is run to the same frequency of 11 Hz (Figure 4b), the salt halo is reduced considerably, which indicates that the elastic effects have a nontrivial impact on the salt boundary sharpness. Besides the sharper salt boundaries, the elastic TLFWI model more clearly shows the velocity contrasts and high-frequency details in both sediment and subsalt areas than its acoustic counterpart.

Improvements in the RTM image from the elastic TLFWI velocity over acoustic TLFWI are generally small and are seen around and below thin salt bodies and steep salt flanks (Figures 4c and 4d). This is because the kinematic differences between acoustic and elastic TLFWI models are mostly small except for the areas around thin salt bodies and steep salt flanks where reduction of the salt halo in the elastic TLFWI model results in better definition of the salt geometry and improved model kinematics for subsalt imaging. For higher-frequency FWI runs, say, 15 Hz and above, these migration differences are even smaller because high wavenumber inversion has smaller impact on the kinematics and can hardly manifest itself through conventional migration. RTM images using both acoustic and elastic TLFWI models still suffer from more apparent issues such as poor illumination and swing noises in subsalt regions, and it is difficult for it to reveal this level of subtle improvements from elastic TLFWI.

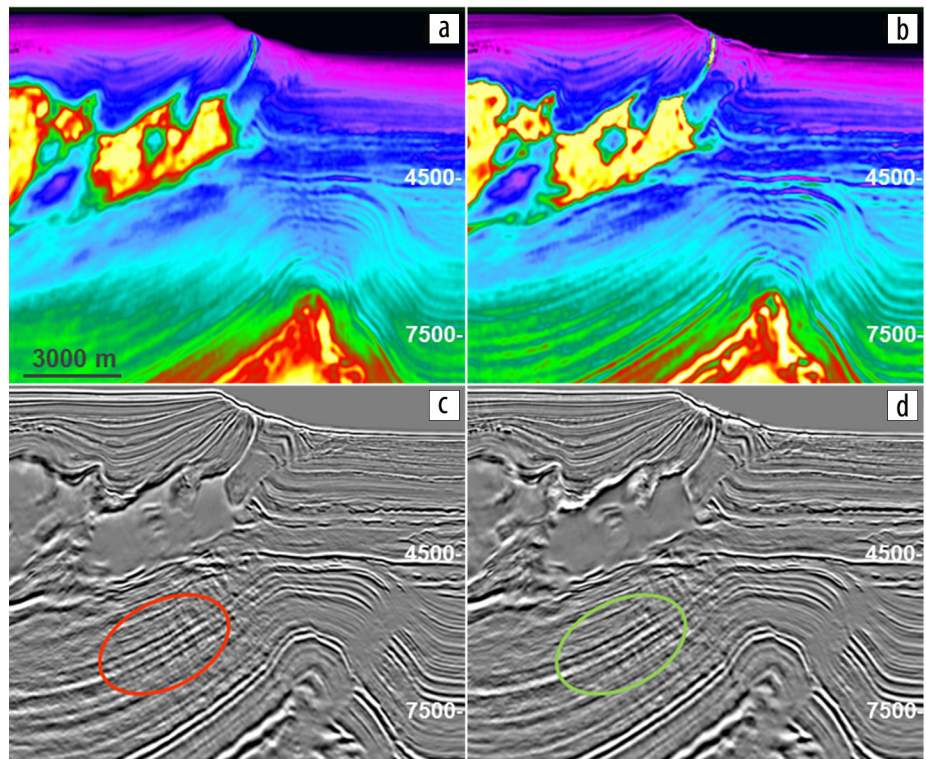


**Figure 4.** Section view of (a) 11 Hz acoustic TLFWI velocity model, (b) 11 Hz elastic TLFWI velocity model, (c) 20 Hz RTM image migrated with acoustic TLFWI velocity in (a), and (d) 20 Hz RTM image migrated with elastic TLFWI model in (b).

Compared to the overall small improvements in RTM images from elastic TLFWI, the uplift in the FDR image directly derived from the FWI velocity model is much more dramatic. This uplift is clearly seen in the data quality maps at the main reservoir generated from these data sets. The subsalt S/N improvements are significant going from RTM to FDR images (Figures 5a and 5b, respectively). Extrasalt areas also show improvement with an increase in S/N and better fault imaging.

The fact that the acoustic wave equation cannot model the dynamic wavefield accurately in a high-contrast solid medium leads to considerable salt halos in acoustic TLFWI outputs, even at 18 Hz, as seen in Figure 6. Elastic TLFWI at the same frequency reduces the salt halo and the ambiguity of the salt sediment boundary (Figure 6). Furthermore, the elastic TLFWI velocity

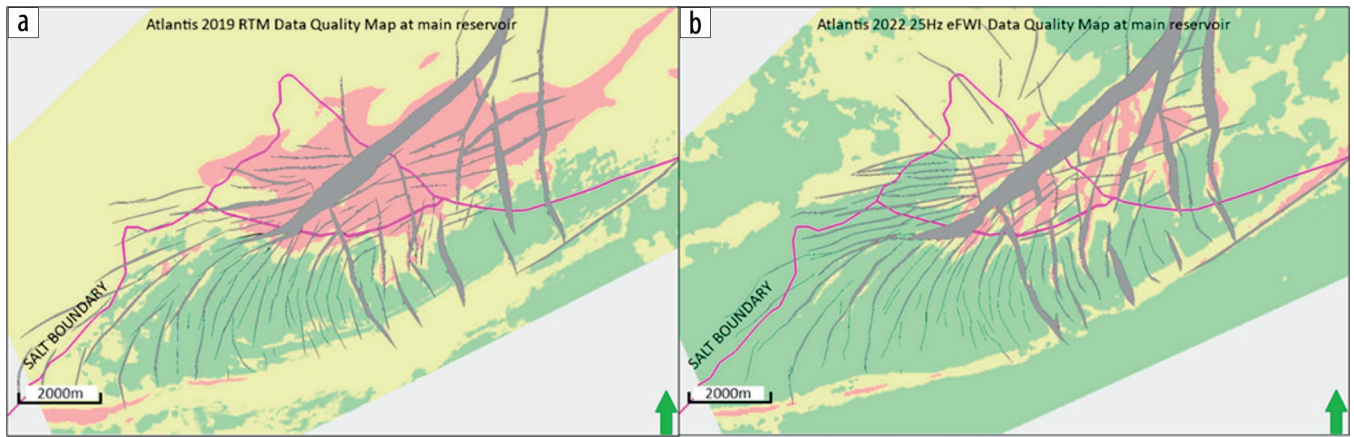


**Figure 5.** Data quality maps showing the interpretability of seismic data at main reservoir. (a) Atlantis 2019 RTM data quality map and (b) Atlantis 2022 25 Hz elastic TLFWI data quality map. Colors represent decreasing S/N going from green to yellow to red.

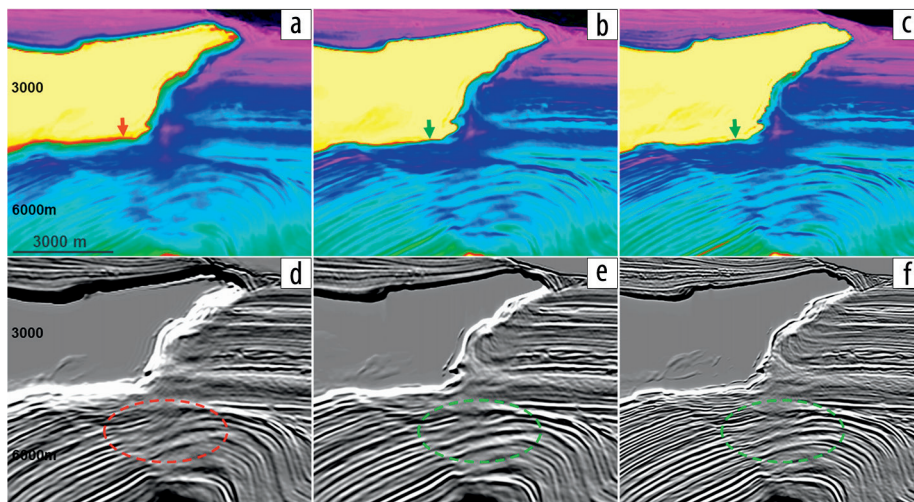


**Figure 6.** Section view of velocity models and FDR images at Atlantis north: (a) 18 Hz acoustic TLFWI velocity model, (b) 18 Hz elastic TLFWI velocity model, and (c) 25 Hz elastic TLFWI model; (d) 18 Hz acoustic FDR image, (e) 18 Hz elastic FDR image, and (f) 25 Hz elastic FDR image.

model shows better velocity contrasts and more details in the sediment and subsalt areas. The resulting elastic FDR image has improved event continuity and higher S/N throughout the entire section. The main reservoir reflectors in the elastic FDR image can be easily interpreted from the subsalt to sediment area. When running to an even higher frequency of 25 Hz, elastic TLFWI further sharpens the image, including the salt boundary, and reveals finer details that were not resolved in the 18 Hz velocity model and FDR image (Figures 6c and 6f).

The improved image quality of the elastic FDR image might be best observed from the frequency decomposition images with RGB color blending. The RGB-blended volume extracted on the major reservoir surface using the raw RTM image shows strong swing noise in the low-illuminated subsalt area (blue ellipse in Figure 7a), consistent with the observations in the RTM images, while the RGB map of the acoustic FDR image shows a reduction of this noise (yellow ellipse in Figure 7b). Moving to the elastic FDR images, the RGB map not only shows further improvements in S/N but also reveals some fine structures interpreted to be faults

(green arrows in Figure 7c). In the sediment area where the S/N is overall reasonable across all images, details such as the fault planes (red, yellow, and green arrows in Figure 7) are also better defined in the FDR image than in the RTM image. While here we compare RTM with FDR, other authors (Huang et al., 2021) have made similar observations when comparing FDR with least-squares RTM.

Conventional imaging products such as Kirchhoff or high-frequency RTM are normally our standard products for high-resolution images, especially for simpler sediment areas. However, in the extrasalt area of Atlantis, the conventional imaging products such as 25 Hz RTM image are not able to resolve the weaker secondary reservoir reflector that

is a consistent development target for the team (Figure 8a). When investigating this area on the 25 Hz elastic FDR image, it was apparent that this weaker reflector was resolvable both in depth and approximate thickness (Figure 8b) and conformed to well logs. Furthermore, the fault planes have proven to be better resolved and more accurately positioned in the 25 Hz elastic FDR image than in the RTM stack, impacting wells in the rig schedule by improving the placement of wells and mitigating the risk of penetrating a faulted-out portion the reservoir. It is noted that the inversion frequency of FDR imaging needs to be high enough to better resolve such detailed reservoir structures. As we observed in Atlantis, a lower-frequency FDR image, e.g., 20 Hz, is still not enough to fully resolve such weak and thin reflectors.

### Improvements in time-lapse (4D) seismic data quality from elastic TLFWI

In Atlantis, time-lapse (4D) seismic surveys have been invaluable surveillance tools for understanding the hydrocarbon habitat and water movement in the reservoirs, understanding

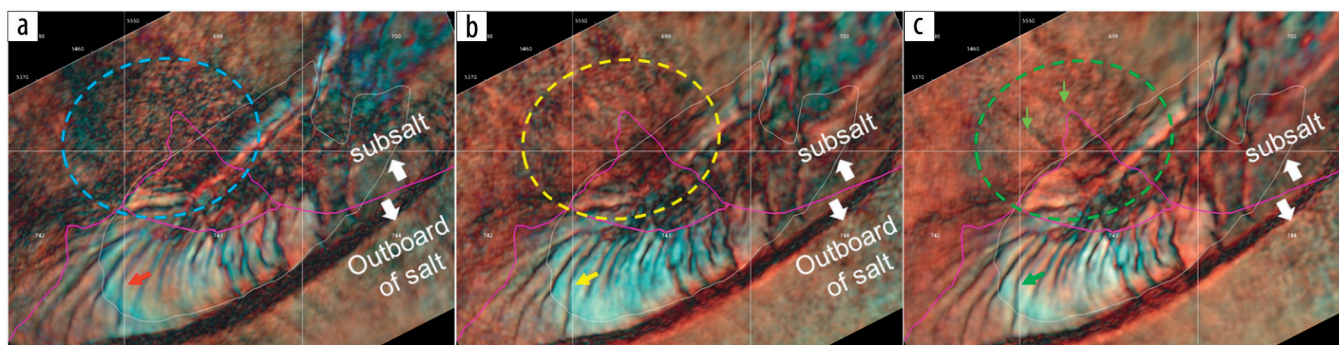


**Figure 7.** Frequency decomposition and RGB-blended maps extracted from various stacks on a major reservoir of Atlantis: (a) 20 Hz RTM, (b) 18 Hz acoustic FDR image, and (c) 18 Hz elastic FDR image. Elastic FDR image shows higher S/N in subsalt and better delineated fault outboard of salt.

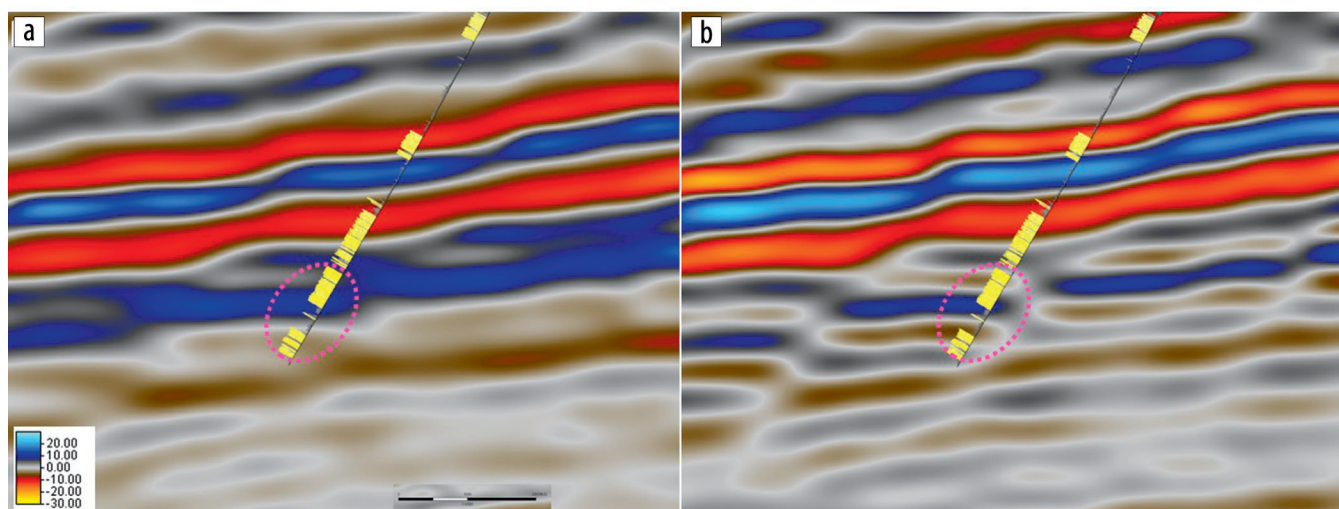


**Figure 8.** Section view of Atlantis images along well trajectory in extrasalt area: (a) 25 Hz RTM image migrated with elastic TLFWI model and (b) 25 Hz elastic FDR image. The high-resolution 25 Hz elastic FDR image is able to resolve the weak secondary reservoir.

reservoir depletion, and for robust placement and sequencing of future production and injection wells. The initial preproduction baseline survey for the field was acquired in 2005. This was followed by four monitor surveys in 2009, 2015, 2019, and 2022. The time-lapse data show clear softening and hardening signals in the three main reservoirs in Atlantis. The observed softening is primarily due to pressure depletion from production, while the hardening response is primarily from aquifer and injected waterfront movement.

Because 3D image quality is still the main driver for 4D data quality, Atlantis 4D imaging results suffer from the same imaging and illumination challenges that also affect the 3D data. Hence, the areas of the field with poor 3D seismic image also have poor 4D seismic response. Prior to 2016 when FWI became the primary tool for updating the Atlantis velocity model for the final 4D migration, the 4D data had little to no usable 4D signal in the subsalt areas of the field. Since 2019, the use of FWI has driven the most improvements to date in 4D data quality (van Gestel, 2021). We have also seen an uplift in subsalt 4D signal by going from acoustic TLFWI to elastic TLFWI for the RTM production 4D migration. This is because even though the improved high-wavenumber content of elastic

TLFWI velocity has only a small impact on the 3D RTM image, the 4D time-lapse responses are more sensitive to such velocity improvements, resulting in a noticeable uplift in the 4D data quality especially in subsalt areas. Figures 9a and 9d show 4D RTM amplitude extractions on the main reservoir in Atlantis and highlight the improvements in the 4D RTM image quality by going from acoustic TLFWI to elastic TLFWI. Subsalt amplitude is weaker due to illumination issues in the RTM image, and the 4D RTM image from an acoustic TLFWI model shows weak but observable subsalt production-related 4D response; however, the 4D signal is heavily contaminated by the strong background noise (black ellipses). By contrast, the 4D RTM difference image from the elastic TLFWI velocity model shows a more coherent subsalt 4D signal and, hence, a more continuous hardening response subsalt (indicated by green arrows). In the extrasalt areas, we also see higher S/N, improved coherency, and better 4D signals from the RTM image with an elastic TLFWI model.

Even with the improvements in the 4D data quality from elastic TLFWI, in most of the northern subsalt areas of Atlantis we still can only see the hardening signal right above the original oil-water contact. The data show no coherent hardening signal

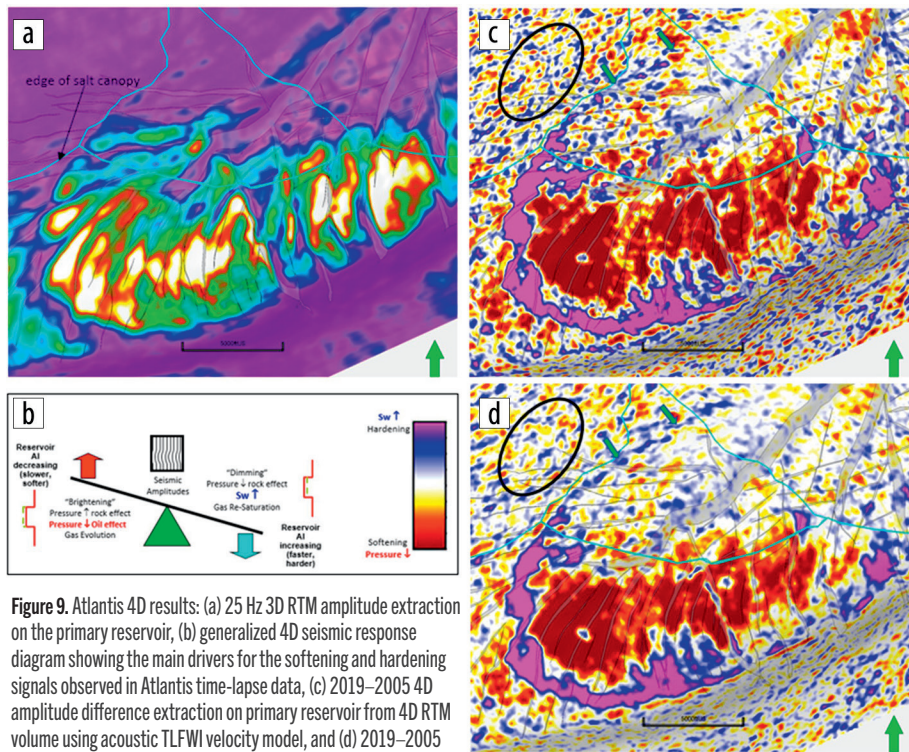


**Figure 9.** Atlantis 4D results: (a) 25 Hz 3D RTM amplitude extraction on the primary reservoir, (b) generalized 4D seismic response diagram showing the main drivers for the softening and hardening signals observed in Atlantis time-lapse data, (c) 2019–2005 4D amplitude difference extraction on primary reservoir from 4D RTM volume using acoustic TLFWI velocity model, and (d) 2019–2005 4D amplitude difference extraction on primary reservoir from 4D RTM volume using elastic TLFWI velocity model.

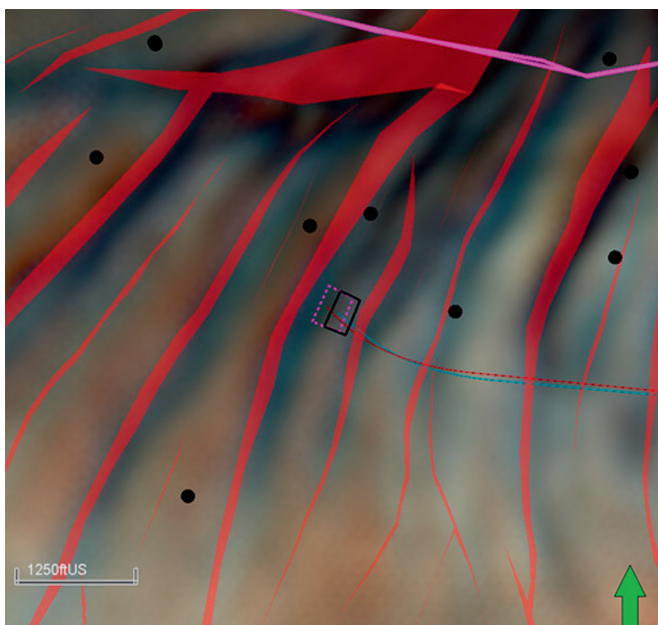


**Figure 10.** Frequency decomposition and RGB-blended map extracted from the main reservoir. Legacy fault polygons are displayed in red. Updated trajectory (blue) and updated target box (black) based on FDR image observations are displayed. Legacy trajectory (red) and legacy target box (blue) are displayed for comparison.

from updip waterfront movement and no coherent softening signal from pressure depletion around the updip producers. To further improve the 4D data quality updip of the original oil-water contact in the northern part of the field and to unlock the full potential of 4D seismic surveillance in the subsalt areas, we expect the use of 4D FDR imaging technology could help.

## Elastic TLFWI imaging impacts on Atlantis development

Leveraging an improved seismic view of the subsurface from the elastic FDR image, the development team has been able to reduce drilling cost by mitigating the risk of penetrating unidentified structural features such as faults, improve commercial value by maximizing reservoir thickness through more accurate targeting, and expand the overall resources of the targets in the well hopper by revealing locations with potential resources from secondary reservoirs.

From the structural and stratigraphic interpretation of the field using FDR images, reservoir surfaces and faults have attained improved lateral and vertical positioning in comparison to the legacy interpretation from the conventional migrated seismic data. These improvements are leveraged to impact the wells in the rig schedule by optimizing the positioning of the target boxes by avoiding mapped faults on the FDR image, thus mitigating

the risk of faulting out the reservoirs. The analysis of spectral decomposition for one of the main reservoirs from the FDR image is used to optimize the location of the target box (Figure 10). The lateral shifts eastward of the fault interpretation from the spectral decomposition in comparison to the legacy fault polygons from conventional migrated seismic data (red) are evident, and these observations were used to update the target boxes and well trajectory.

Secondary reservoirs that were difficult to image in conventionally migrated seismic images — for example, Figure 8a — have seen improvement in vertical/lateral resolution and amplitude fidelity with the FDR image. These improvements have allowed the development team to reveal locations with potential resources using seismic attribute analysis techniques such as amplitude and velocity extractions from the secondary reservoir and integrating observations with well penetrations. The velocity extraction map from a secondary reservoir displays a correlation between the fluid of the well penetrations and velocity values (Figure 11). A correlation of lower velocity values and locations of hydrocarbon penetrations is evident. Such observations are used to predict additional areas where hydrocarbons could be present, thus revealing new targets and expanding opportunities in the hopper and increasing the life of the field.

## Discussion

To optimally focus the seismic energy in the complex subsurface salt environment of Atlantis, an accurate velocity model has shown to be the most crucial factor. Coupling this with state-of-art elastic TLFWI and FDR imaging provides the most accurate

reservoir images to date, allowing the development team to not only increase their confidence in the interpretation and field development throughout the low-illuminated subsalt areas but also resolve the smaller structural details such as faults placement and weaker secondary reservoir reflectors in extrasalt locations, enabling more precise well placement for a successful realization of the future potential at Atlantis.

These improvements would not be possible without the high-quality OBN data. In Atlantis, the 2015 OBN data with long offset (up to 35 km), full-azimuth, and good low-frequency S/N provide reasonable constraints for the low-wavenumber velocity model update to correct the complex salt model errors in areas such as salt fingers and sediment inclusions. Whereas for the high-wavenumber details coming from higher-frequency FWI, denser nodes that adequately sample the complex wavefield and offer a higher stacking power are key to further improvements, especially at the poorly illuminated subsalt areas. As evident in Figures 12a–12d, running elastic TLFWI from 20 to 25 Hz with 2019 OBN with node spacing of  $200 \times 400$  m increases the image resolution throughout the section, but it also introduces noticeable noise to the subsalt image in areas of poor illumination, which can compromise the accurate interpretation of reservoir details and defeat the purpose of running higher-frequency inversion. In comparison, the 25 Hz FDR image using the densified 2022 OBN (Figures 12c and 12f) with node spacing of  $200 \times 200$  m improved the S/N at the low-illuminated subsalt area without adding adverse noise. Tests with 2022 OBN for an even higher-

frequency FDR image are ongoing to fully explore the benefits of this dense OBN data.

Looking ahead, seeing the advantages of elastic FDR imaging in improving the illumination and S/N in the 3D subsalt image at Atlantis Field, it is natural to extend the elastic FDR imaging

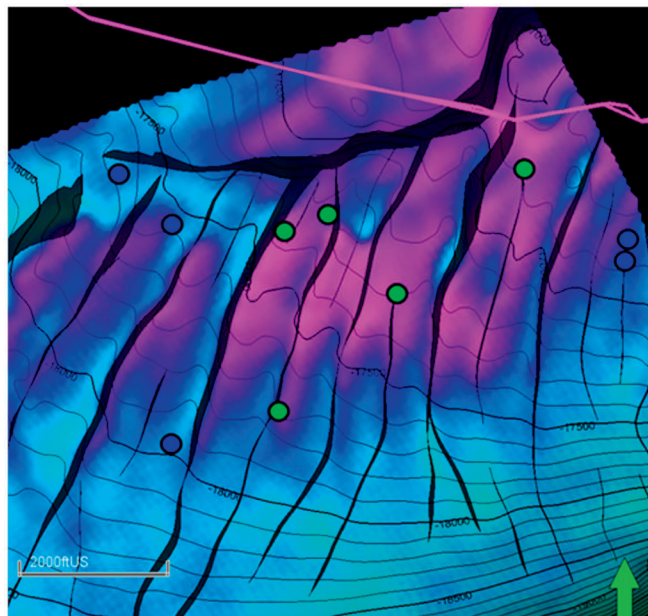


Figure 11. Velocity extraction map of a secondary reservoir. Penetrations of hydrocarbons are displayed in green, and penetrations of brine are displayed in blue.

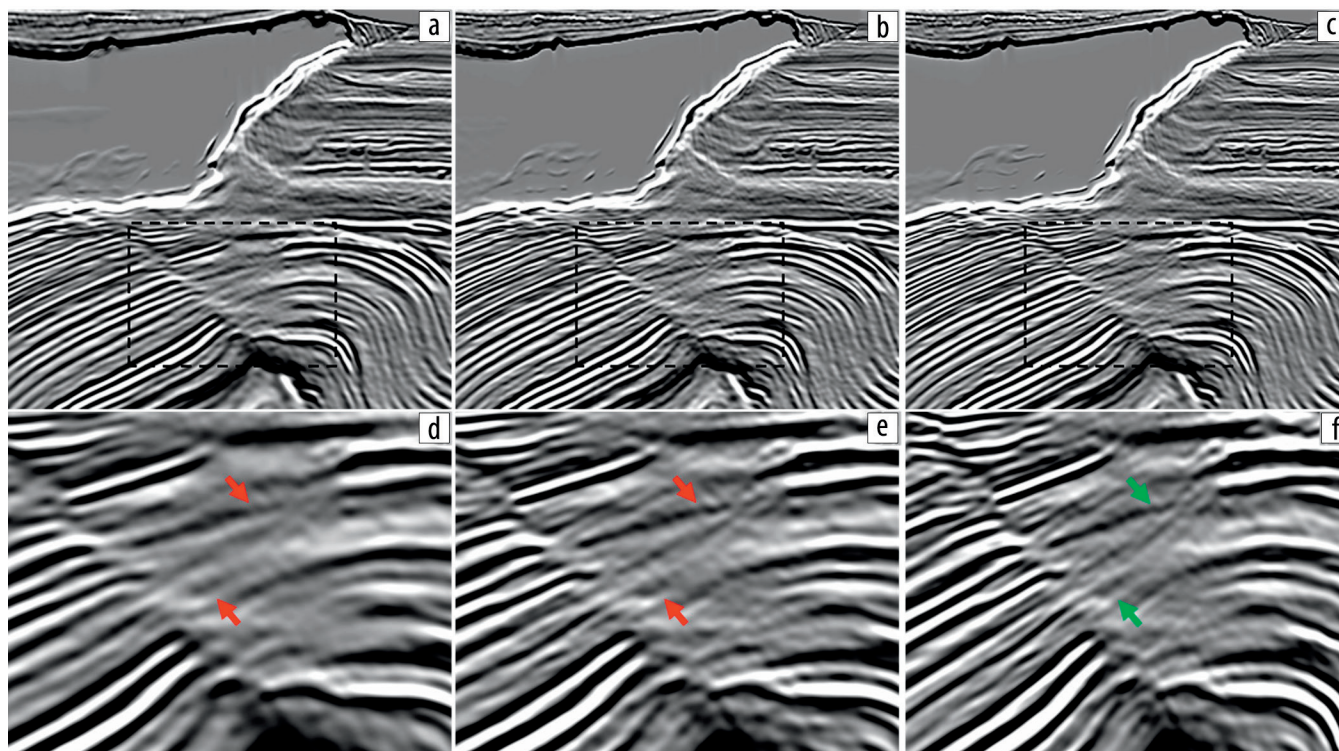


Figure 12. Section view of high-frequency elastic FDR images using different node density OBN data: (a) 20 Hz elastic FDR image using  $200 \times 400$  m node spacing OBN, (b) 25 Hz elastic FDR image using  $200 \times 400$  m node spacing OBN, and (c) 25 Hz elastic FDR image using  $200 \times 200$  m node spacing OBN. Panels (d)–(f) are the zoomed-in display in the dashed rectangle in (a)–(c), respectively. FDR images using denser OBN data have higher S/N at higher frequencies.

from 3D to 4D for better subsalt 4D responses. Current 4D results using RTM show weaker 4D amplitude and poor S/N in subsalt regions due to low illumination in those areas. Time-lapse elastic FDR imaging provides the potential to compensate for the low subsalt illumination and improve the subsalt 4D S/N over RTM results.

## Conclusion

High-frequency elastic TLFWI and FDR imaging can extract maximum value from the existing Atlantis Field data. This provides a clearer path to effectively resolving the remaining challenges in the field's imaging shortcomings, which in turn brings significant uplift to reservoir understanding over previous algorithms. Elastic TLFWI largely reduces the salt halo observed in acoustic TLFWI velocity and sharpens the velocity contrasts, improving the details over the acoustic TLFWI velocity model. This has led to extraordinary resolution and reservoir details that were not observed before at Atlantis. Although relatively small improvements are observed in the kinematics for 3D structural imaging, elastic TLFWI provides noticeable uplifts in the 4D difference plots even when employing RTM images. After the initial breakthrough of automated FWI salt model building, which led to a step change of the reservoir imaging at Atlantis in the last decade, elastic TLFWI and FDR imaging provided another leap in imaging the field. **TLE**

## Acknowledgments

We thank BP, Woodside Energy, and CGG for permission to publish this work. We are grateful for joint efforts of generations of geophysicists and geologists on Atlantis from BP, Woodside, and CGG.

## Data and materials availability

Data associated with this research are confidential and cannot be released.

Corresponding author: sam.buist@bp.com

## References

Beaudoin, G., and A. A. Ross, 2007, Field design and operation of a novel deepwater, wide-azimuth node seismic survey: *The Leading Edge*, **26**, no. 4, 494–503, <https://doi.org/10.1190/1.2723213>.  
 Brenders, A., J. Dellinger, I. Ahmed, E. Díaz, M. Gherasim, H. Jin, M. Vyas, and J. Naranjo, 2022, The Wolfspär experience with low-frequency seismic source field data: Motivation, processing, and implications: *The Leading Edge*, **41**, no. 1, 9–18, <https://doi.org/10.1190/tle41010010.1>.

Dellinger, J., A. Ross, D. Meaux, A. Brenders, G. Gesoff, J. Etgen, J. Naranjo, G. Openshaw, and M. Harper, 2016, Wolfspär®, an “FWI-friendly” ultralow-frequency marine seismic source: 86<sup>th</sup> Annual International Meeting, SEG, Expanded Abstracts, 4891–4895, <https://doi.org/10.1190/segam2016-13762702.1>.  
 Elebiju, B., Q. Li, K. Hartman, F. Rollins, Y. Feng, K. Kaiser, W. Schinagl, et al., 2022, One more stride forward in Thunder Horse subsalt imaging with elastic FWI: Second International Meeting for Applied Geoscience & Energy, SEG/AAPG, Expanded Abstracts, 947–951, <https://doi.org/10.1190/image2022-3750987.1>.  
 Huang, R., Z. Zhang, Z. Wu, Z. Wei, J. Mei, and P. Wang, 2021, Full-waveform inversion for full-wavefield imaging: Decades in the making: *The Leading Edge*, **40**, no. 5, 324–334, <https://doi.org/10.1190/tle40050324.1>.  
 Lewis, B., M. Pfister, C. Brooks, G. Astvatsaturov, and S. Michell, 2016, Efficient acquisition of deepwater node surveys: 86<sup>th</sup> Annual International Meeting, SEG, Expanded Abstracts, 92–96, <https://doi.org/10.1190/segam2016-13867668.1>.  
 Michell, S., X. Shen, A. Brenders, J. Dellinger, I. Ahmed, and K. Fu, 2017, Automatic velocity model building with complex salt: Can computers finally do an interpreter's job?: 87<sup>th</sup> Annual International Meeting, SEG, Expanded Abstracts, 5250–5254, <https://doi.org/10.1190/segam2017-17778443.1>.  
 Shen, X., I. Ahmed, A. Brenders, J. Dellinger, J. Etgen, and S. Michell, 2017, Salt model building at Atlantis with full-waveform inversion: 87<sup>th</sup> Annual International Meeting, SEG, Expanded Abstracts, 1507–1511, <https://doi.org/10.1190/segam2017-17738630.1>.  
 van Gestel, J., 2021, Ten years of time-lapse seismic on Atlantis Field: *The Leading Edge*, **40**, no. 7, 494–501, <https://doi.org/10.1190/tle40070494.1>.  
 Wang, P., Z. Zhang, J. Mei, F. Lin, and R. Huang, 2019, Full-waveform inversion for salt: A coming of age: *The Leading Edge*, **38**, no. 3, 204–213, <https://doi.org/10.1190/tle38030204.1>.  
 Wei, Z., J. Mei, Z. Wu, Z. Zhang, R. Huang, and P. Wang, 2023, Pushing seismic resolution to the limit with FWI imaging: *The Leading Edge*, **42**, no. 1, 24–32, <https://doi.org/10.1190/tle42010024.1>.  
 Wu, Z., Z. Wei, Z. Zhang, J. Mei, R. Huang, and P. Wang, 2022, Elastic FWI for large impedance contrasts: Second International Meeting for Applied Geoscience & Energy, SEG/AAPG, Expanded Abstracts, 3686–3690, <https://doi.org/10.1190/image2022-w17-02.1>.  
 Zhang, Z., J. Mei, F. Lin, R. Huang, and P. Wang, 2018, Correcting for salt misinterpretation with full-waveform inversion: 88<sup>th</sup> Annual International Meeting, SEG, Expanded Abstracts, 1143–1147, <https://doi.org/10.1190/segam2018-2997711.1>.  
 Zhang, Z., Z. Wu, Z. Wei, J. Mei, R. Huang, and P. Wang, 2020, FWI imaging: Full-wavefield imaging through full-waveform inversion: 90<sup>th</sup> Annual International Meeting, SEG, Expanded Abstracts, 656–660, <https://doi.org/10.1190/segam2020-3427858.1>.  
 Zhang, Z., Z. Wu, Z. Wei, J. Mei, R. Huang, and P. Wang, 2023, Enhancing salt model resolution and subsalt imaging with elastic FWI: *The Leading Edge*, **42**, no. 3, 207–215, <https://doi.org/10.1190/tle42030207.1>.